A Remote Sensing Model to Estimate Sunshine Duration in the Ningxia Hui Autonomous Region, China

ZHU Xiaochen[1] (朱晓晨), QIU Xinfa[1*] (邱新法), ZENG Yan[2] (曾 燕), GAO Jiaqi[3] (高佳琦), and HE Yongjian[1] (何永健)

1 *School of Remote Sensing, Nanjing University of Information Science & Technology, Nanjing* 210044

2 *Jiangsu Institute of Meteorological Sciences, Jiangsu Meteorological Bureau, Nanjing* 210008

3 *College of Atmospheric Science, Nanjing University of Information Science & Technology, Nanjing* 210044

(Received April 30, 2014; in final form September 28, 2014)

ABSTRACT

Sunshine duration (SD) is strongly correlated with solar radiation, and is most widely used to estimate the latter. This study builds a remote sensing model on a 100 m × 100 m spatial resolution to estimate SD for the Ningxia Hui Autonomous Region, China. Digital elevation model (DEM) data are employed to reflect topography, and moderate-resolution imaging spectroradiometer (MODIS) cloud products (Aqua MYD06_L2 and Terra MOD06_L2) are used to estimate sunshine percentage. Based on the terrain (e.g., slope, aspect, and terrain shadowing degree) and the atmospheric conditions (e.g., air molecules, aerosols, moisture, cloud cover, and cloud types), observation data from weather stations are also incorporated into the model. Verification results indicate that the model simulations match reasonably with the observations, with the average relative error of the total daily SD being 2.21%. Further data analysis reveals that the variation of the estimated SD is consistent with that of the maximum possible SD; its spatial variation is so substantial that the estimated SD differs significantly between the south-facing and north-facing slopes, and its seasonal variation is also large throughout the year.

Key words: sunshine duration, digital elevation model data, moderate-resolution imaging spectroradiometer (MODIS), cloud cover, remote sensing estimation model

Citation: Zhu Xiaochen, Qiu Xinfa, Zeng Yan, et al., 2015: A remote sensing model to estimate sunshine duration in the Ningxia Hui Autonomous Region, China. *J. Meteor. Res.*, **29**(1), 144–154, doi: 10.1007/s13351-015-4059-1.

1. Introduction

Sunshine duration (SD) is an important indicator of the amount of solar radiation received in a region. Adequate sunshine not only increases air temperature and effective accumulated temperature but also aids photosynthesis in plants, thereby promoting their growth. SD is the most visible manifestation of solar radiation (Watson and Albritton, 2001), and it is strongly correlated with solar radiation (Takenaka, 1988; Ertekin and Evrendilek, 2007). As a result, SD is the most widely used parameter to estimate solar radiation (Yin, 1957; Weng, 1964; Şen, 2001; Şen and Öztopal, 2003). Many empirical models for the prediction of solar radiation from SD have been developed (Angstrom, 1924; Ertekin and Evrendilek, 2007). SD is also an important parameter in the study of ecosystem process models, hydrological simulation models, and biophysical models (Weng, 1997).

SD is affected by terrain factors (e.g., slope, aspect, and terrain shadowing degree) and atmospheric factors (e.g., air molecules, aerosols, moisture, cloud cover, and cloud types). Here, we use digital elevation model (DEM) data to comprehensively reflect the terrain. These data (with different resolutions) have unique abilities to reflect and characterize terrain. However, due to certain restrictions (e.g., computation speed and model efficiency), the calculation

Supported by the National Natural Science Foundation of China (41175077) and Jiangsu Innovation Program for Graduate Education (CXZZ12_0506).

*Corresponding author: xfqiu135@nuist.edu.cn.

model is rarely applied to DEM data on the 1:250000 scale in large-scale distribution modeling research (Li et al., 2008). Additionally, we use the sunshine percentage estimated from the moderate-resolution imaging spectroradiometer (MODIS) cloud products (the Aqua MYD06_L2 and the Terra MOD06_L2) to comprehensively reflect the atmosphere because clouds strongly affect the solar radiation on the earth's surface (Suehrcke et al., 2013). The sunshine percentage is also known as the sunshine fraction, i.e., the ratio between the actual sunshine duration and the possible sunshine duration. The possible sunshine duration must be measured on a day that is entirely cloudless.

SD is calculated by using the maximum possible SD (MPSD) and sunshine percentage. Traditionally, the calculation of SD has been achieved by three major methods: the empirical equation method (Wang, 1993), the analytical method (Fu, 1958; Zhu, 1988), and the graphical method (Weng et al., 1981; Sun and Fu, 1996). With the development of space technology, many researchers have tried to improve the simulation accuracy with regard to the calculation of SD. The simulation accuracy of the portion of the MPSD used in the calculation of SD was improved with the development and promotion of the DEM (Moore et al., 1991). Dozier and Outcalt (1979) proposed that using the DEM to simulate solar radiation enabled a digital approach to explore the effect of terrain on the MPSD. Hetrick et al. (1993), Dubayah et al. (1990), Kumar et al. (1997), and Bocquet (1984) studied the MPSD in mountains with regard to the influence of terrain on solar radiation by applying the geographic information system (GIS). Zeng et al. (2003) investigated the spatial distribution of MPSD in China using data at a spatial resolution of 1 km × 1 km by establishing a distribution model for MPSD in rugged terrains. Chen et al. (2002) and Yuan et al. (2008) used the sunshine percentage from the routine observation data at weather stations to calculate the actual SD in specific research areas. Some researchers have attempted to estimate SD from satellite data, which provide better spatial coverage and representation (Good, 2010; Shamim et al., 2012; Bertrand et al., 2013). Shamim et al. (2012) presented an improved model for global SD estimation. The methodology incorporated geostationary satellite images by including snow cover information, sun and satellite angles, and a trend correction factor for seasons for the determination of cloud cover index.

Based on previous studies, we now consider the effects of both terrain and atmospheric factors by using the DEM data for the Ningxia Hui Autonomous Region (abbreviated as Ningxia hereafter) to establish a distribution model of MPSD and by using the 2003 daily MODIS cloud products to construct a remote sensing estimation model for sunshine percentage. As a result, we completed the estimation of SD in Ningxia based on the MODIS cloud cover data. Section 2 describes the climate of Ningxia. Section 3 describes the data used in the current study and the primary methods. Section 4 presents a systematic analysis of the SD estimation results. The discussion and conclusions are presented in Sections 5 and 6, respectively.

2. Climatic conditions in Ningxia, China

Ningxia is located in 35°14′–39°23′N, 104°17′–107°39′E, and its capital city, Yinchuan, is located in the center of the region, upstream of the Yellow River in western China. This region spans 456 km north to south and 250 km west to east, covering an area of approximately 66000 km^2.

Two climates occur in Ningxia: the eastern monsoon climate and the northwest arid climate. The region is close to the Qinghai-Tibetan alpine area, placing it approximately at the transition zone of three natural regions: the eastern monsoon region, the northwest arid and semiarid region, and the Qinghai-Tibetan alpine region. According to historical records of standard weather stations, the annual average temperature of Ningxia is approximately 8.2℃, and the average annual rainfall is approximately 272.6 mm.

3. Data and methods

3.1 Data

The data used for this study consist of:

(1) Observations obtained by weather stations in

Ningxia, including the monthly average total cloud cover and low cloud cover, and SD observed from standard weather stations in 2003, as well as the monthly average SD at the intensive observation stations during the same year. The observational data at the standard weather stations are used to develop the remote sensing model for estimating the SD, and the data from the intensive observation weather stations are used to assess the model error. These data are provided by the National Meteorological Information Center of the China Meteorological Administration and are subjected to strict quality control. Figure 1 presents a distribution map of standard and intensive observation weather stations in Ningxia.

(2) Satellite remote sensing data, including the daily TERRA/MODIS (MOD06_L2) and the Aqua/MODIS (MYD06_L2) cloud data for Ningxia and its surrounding regions in 2003, with a spatial resolution of 5 km × 5 km. These data are obtained from the TERRA/MODIS and Aqua/MODIS image total daily cloud cover data by using a geometric correction → image mosaic → total daily cloud cover image superposition procedure. Due to movement of the sensing platform, undulating terrain, curvature of the earth's surface, atmospheric refraction, and the earth's rotation, the remote sensing image distortion occurs for a given geometric position. Through geometric correction, such problems can be solved. Due to changes in the scanning position, the cloud cover of the study area is distributed over multiple sets of images. An image mosaic is constructed by splicing a series of flat images together to create a continuous panoramic image. The cloud cover for 15 April 2003 was obtained by using geometric correction, image mosaic, and cloud cover image superposition, as shown in Fig. 2.

(3) National basic geographic data, including the DEM (100 m × 100 m) data for Ningxia, an administrative map of Ningxia, and basic geographic informa-

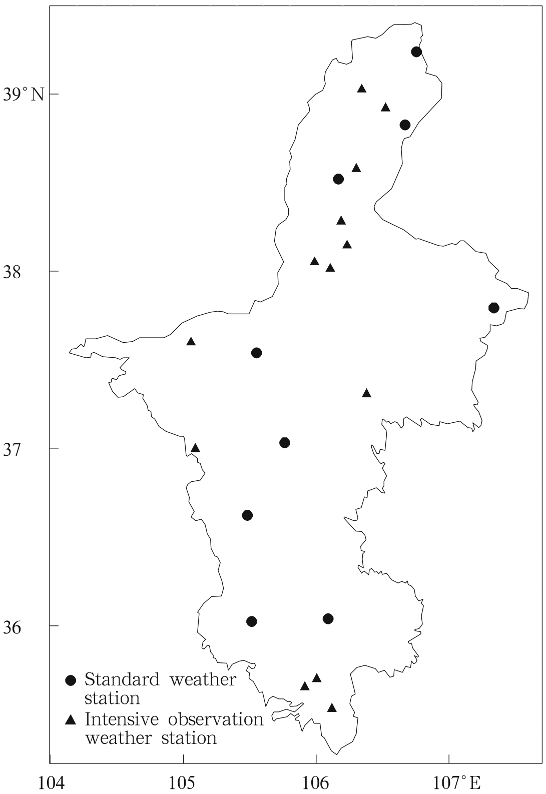

Fig. 1. Distribution of the standard and intensive observation weather stations in Ningxia.

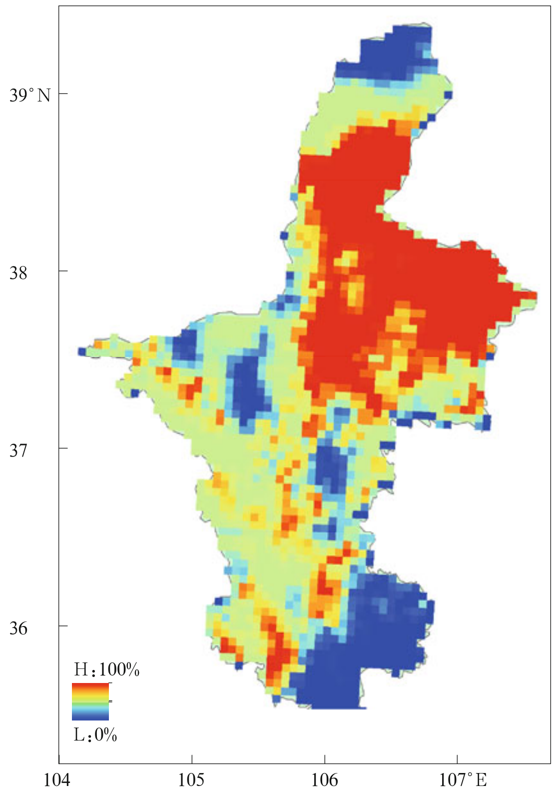

Fig. 2. The cloud cover over Ningxia on 15 April 2003, obtained by using geometric correction, image mosaic, and a cloud cover image superposition procedure.

tion collected from the standard and intensive observation weather stations.

The data used for this study are subjected to rigorous quality control. The software used for data analysis includes SPSS (Statistical Package for the Social Sciences), Access database, ArcGIS (the Environmental Systems Research Institute, Inc.'s geographic information software), and ENVI (Environment for Visualizing Images) remote sensing image processing software. In this study, ENVI is used for remote sensing image analysis and display, SPSS is used for statistical analysis of the data, and ArcGIS is used for the projection and its secondary development.

3.2 Methods

3.2.1 The sunshine percentage estimation model

Previous studies (e.g., Liu et al., 2009) have demonstrated that there is always some deviation between the satellite-retrieved cloud data and the total cloud data observed at weather stations; thus, it is necessary to correct the satellite-retrieved cloud data before they are used. Cao et al. (2012) proposed five correction methods for the MODIS cloud product with ground observation data, of which the ratio method showed the best correction results. A linear relationship exists between the sunshine percentage and the cloud cover, and the latter is the primary factor that affects the variation of the former (Ding et al., 2005). Recently, Matuszko (2012) also analyzed the influence of cloudiness on SD. The major factors that affect sunshine percentage include low and total cloud cover, which are corrected by the ratio method. Taking these effects on sunshine percentage into consideration, we established a remote sensing estimation model for sunshine percentage as follows.

$$\mathrm{SR_g} = a + b \cdot \mathrm{CL_p} + c \cdot \mathrm{Low_p}, \tag{1}$$

$$\mathrm{SR} = \mathrm{interpolate}(a) + \mathrm{interpolate}(b) \cdot \mathrm{CL} + \mathrm{interpolate}(c) \cdot \mathrm{Low}, \tag{2}$$

where $\mathrm{SR_g}$ represents the sunshine percentage observed at the weather station; $\mathrm{CL_p}$ is the total cloud cover at the pixel corresponding to the weather station location; $\mathrm{Low_p}$ is the low cloud cover data at the pixel corresponding to the weather station location; a, b, and c are regression coefficients; interpolate () represents the interpolation result of a, b, and c; SR is the sunshine percentage image data; CL is the total set of cloud image data after correction; and Low represents the low cloud cover image data after correction.

The sunshine percentage estimation process includes the following steps. First, calculate the monthly mean MODIS cloud cover based on the daily data. Second, revise the MODIS total cloud cover image based on the monthly total cloud cover reported by ground observations and the monthly mean MODIS cloud cover by using the ratio correction method. Third, establish the ratio relationship between total cloud cover and low cloud cover reported by ground observations, and calculate the MODIS low cloud cover image and MODIS total cloud cover image after correction. Fourth, extract the monthly MODIS total and low cloud cover for each meteorological station after correction, establish the linear regression equation between the sunshine percentage reported by ground observations and total and low MODIS cloud cover using Eq. (1), and calculate the monthly coefficients a, b, and c in Eq. (1). Fifth, interpolate the monthly coefficients a, b, and c to obtain the corresponding spatial distribution. Sixth, calculate the sunshine percentage from the image data by raster calculation, according to Eq. (2).

3.2.2 The SD model

In general, two different definitions exist for MPSD: 1) the astronomical MPSD (without taking atmospheric and terrain shading factors into account) and 2) the geographical MPSD (which considers terrain-shading factors without atmospheric effects). The MPSD in this study refers to the geographical MPSD (Zuo, 1990). Studies have shown that the SD at any point in actual rugged terrains for a given day is the product that combines the MPSD for rugged terrains and the sunshine percentage. This model is written as

$$L_{\alpha\beta} = L_{0\alpha\beta} \cdot \mathrm{SR}, \tag{3}$$

where $L_{\alpha\beta}$ is the SD of rugged terrains, and $L_{0\alpha\beta}$ is the MPSD of rugged terrains. $L_{0\alpha\beta}$ is calculated by using the MPSD distribution model developed by Zeng et al. (2003) for rugged terrains, and SR is derived from the sunshine percentage estimate model described in Section 3.2.1. Figure 3 illustrates the calculation procedure for the SD model.

4. Results

4.1 Estimation of sunshine percentage

Based on the computation flow chart in Fig. 3 and Eqs. (1)–(3), we derived the corrected total cloud cover image data, the estimated low cloud cover image data (Cao et al., 2012), and the estimated sunshine percentage image data combined with its associated ground data. The sunshine percentage estimates obtained by using remote sensing are presented in Fig. 4. The overall sunshine percentage in January and October was greater than that in April and July, primarily because sunny days predominated during the fall and winter seasons of 2003 in Ningxia. The sunshine percentage magnitudes are higher in the north than in the south in this case. An error analysis for sunshine percentage is conducted by using 13 intensive observation stations in Ningxia, and the results are presented in Table 1. The maximum monthly average absolute error (MAE) is 8.23% and it occurred in April, and the average absolute error for the entire year of 2003 is relatively small (5.30%).

4.2 Estimation of SD and its seasonal variation

We estimated SD using the aforementioned method. Its estimation results and magnified regional maps are presented in Fig. 5, which clearly demonstrates that the annual average total daily SD in Ningxia in 2003 was distributed with higher values in the north and west than in the south and east. In general, the average total daily SD in 2003 was 7.18 h in Ningxia. The duration was lowest over the southern mountainous area, where the annual average total SD was only 4.3–5.3 h. The second lowest SD was in the southeastern and southwestern mountainous areas, where the annual average daily total SD ranged from 5.2 to 6.4 h. The highest SD was in the northernmost and mid-west of Ningxia, which had an annual average daily total SD of approximately 8.6 h. It can be easily inferred that the regional topography significantly affected the SD, especially in mountainous areas with rugged terrains. The shading effects of slope, aspect, and the surrounding terrains on SD are fully demonstrated here.

January, April, July, and October were chosen to represent winter, spring, summer, and fall, respectively. Figure 6 illustrates spatial distributions of the monthly averaged total daily SD over Ningxia during the four seasons of 2003. In general, the spatial distribution of SD during the four seasons is consistent

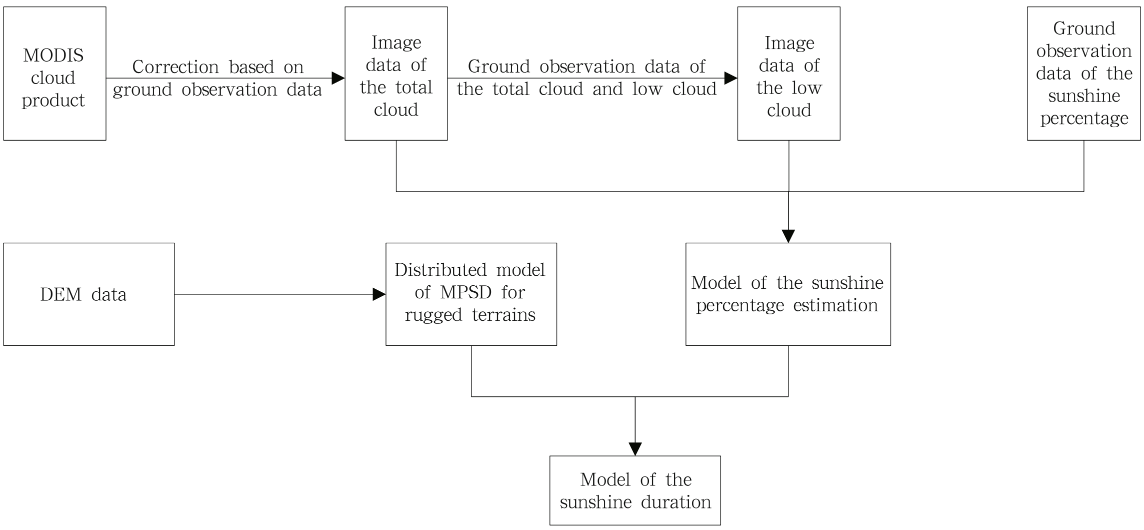

Fig. 3. Flow chart of the calculation procedure for the SD model.

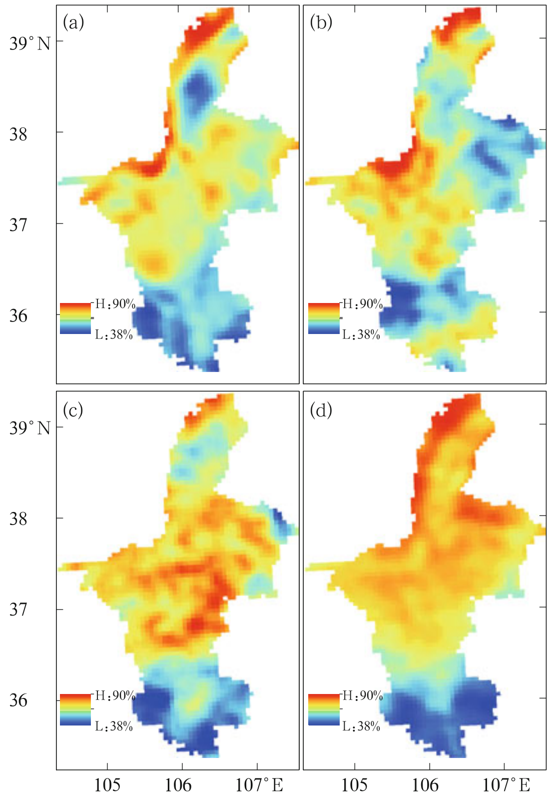

Fig. 4. Sunshine percentage estimates over Ningxia in (a) January, (b) April, (c) July, and (d) October 2003.

with that of the annual SD, with obvious distribution characteristics, e.g., SD is higher in the mid-west than the south, and higher in high-latitude areas than low-latitude areas. The average SDs in Ningxia were 7.25, 7.77, 7.25, and 7.03 h in spring, summer, fall, and winter, respectively. Moreover, SD values decreased in the order: summer > spring > fall > winter; this order reveals an asymmetric SD distribution for the four seasons. The maximum SD appeared in the order as follows: spring > summer > fall > winter. The minimum SD occurred in the following order: summer > spring > fall > winter.

4.3 Model verification

To estimate the accuracy of SD simulation for rugged terrains, we compared the observation data at the 13 intensive observation weather stations in Ningxia with the simulated SD results. This verification mainly focused on two aspects: (1) we verified the error of the interpolation results at the standard stations using the SD data from the intensive observation stations in Ningxia; (2) we verified the error of the SD estimation using the remote sensing method (Fig. 3) at the intensive observation stations. To obtain the value at the grid point corresponding to the latitude and longitude of each weather station, the effect on the errors of the geographic and topographic parameters was considered. The major errors include precision error in the DEM data and weather station location error. Therefore, we adopted a previously described pixel method (Qiu et al., 2009) to extract the data at the grid points corresponding to the weather stations. As Table 2 shows, MAE of SD was 0.39–0.78 h, MRE (monthly average relative error) of SD was 5.41%–11.82%, the annual average absolute error was 0.57 h, and the annual average relative error was approximately 7.9% for the 2003 data in Ningxia, based on the interpolation method at the standard stations and the verification with the observational data at the intensive observation stations. Table 3 lists the SD simulation errors derived by using the intensive station data and the MODIS cloud data. Table 3 also shows that the MAE of SD was 0.10–0.51 h, MRE of SD was 1.47%–8.80%, the annual average absolute error was approximately 0.16 h, and the annual average relative error was approximately 2.21% for the 2003 data in Ningxia. The error in Table 3 was generally much smaller than in Table 2, indicating that the introduction of the MODIS cloud data has increased the accuracy of the SD estimation.

4.4 Sub-regional distributions of SD

To further analyze the effect of the local topography on SD and to highlight the variation of MPSD

Table 1. Error analysis for sunshine percentage estimation at the intensive observation stations in Ningxia during 2003

Month	1	2	3	4	5	6	7	8	9	10	11	12	Average
MAE (%)	4.84	4.45	5.07	8.23	6.20	4.51	4.00	5.94	4.28	3.59	6.12	6.41	5.30

Note: MAE denotes the monthly average absolute error of sunshine percentage.

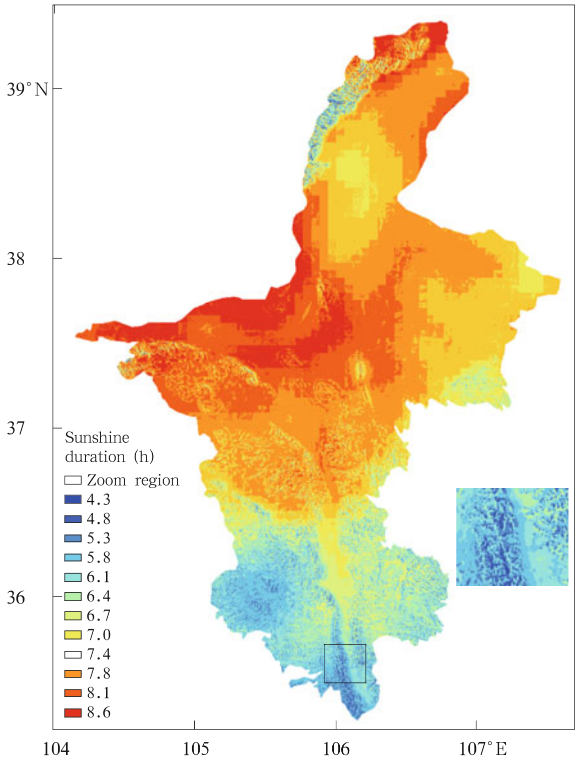

Fig. 5. Annual average distributions of the total daily SD in Ningxia in 2003.

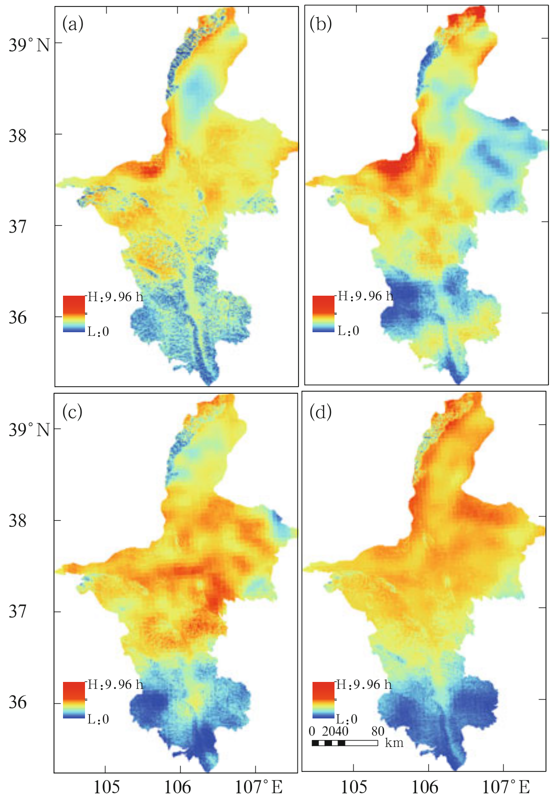

Fig. 6. Monthly average distributions of the total daily SD in Ningxia in (a) January, (b) April, (c) July, and (d) October 2003.

and SD with terrain, we examined the MPSD and SD anomalies, which are the differences between the grid point values for certain terrain aspects and the average of all the grid points for all terrain aspects. The MPSD anomaly variations with terrain aspects for different months are illustrated in Figs. 7a and 7b. The figures show that the MPSD anomalies for the 90°–180° aspect decreased in the order of January > October > April > July, and the order of MPSD anomalies for the 0°–90° and 180°–360° aspects were July > April > October > January. Moreover, the MPSD variation on the 15° southern terrain slope was larger than the 10° slope in January. The SD variation trend illustrated in Figs. 7c and 7d is similar to the trend in Figs. 7a and 7b. The cloud cover anomaly variations with aspects for different months are illustrated in Figs. 7e and 7f. These figures show that in January, the cloud variation is as strong as in other months, and the cloud cover and the terrain have no obvious regularity. In January, the direct sunshine point is located near the

Table 2. Error analysis for the 2003 SD results derived by using the interpolation method based on the station data

Month	1	2	3	4	5	6	7	8	9	10	11	12	Average
MAE (h)	0.46	0.50	0.50	0.78	0.65	0.65	0.75	0.68	0.46	0.39	0.43	0.59	0.57
MRE (%)	5.93	6.72	6.99	9.51	7.13	6.46	11.62	11.82	6.83	5.41	7.63	8.86	7.90

Table 3. Error analysis for the 2003 SD estimates based on the MODIS cloud data

Month	1	2	3	4	5	6	7	8	9	10	11	12	Average
MAE (h)	0.22	0.15	0.10	0.13	0.14	0.13	0.10	0.14	0.10	0.10	0.13	0.51	0.16
MRE (%)	2.89	2.05	1.57	1.62	1.60	1.32	1.32	1.93	1.48	1.29	2.28	7.27	2.21

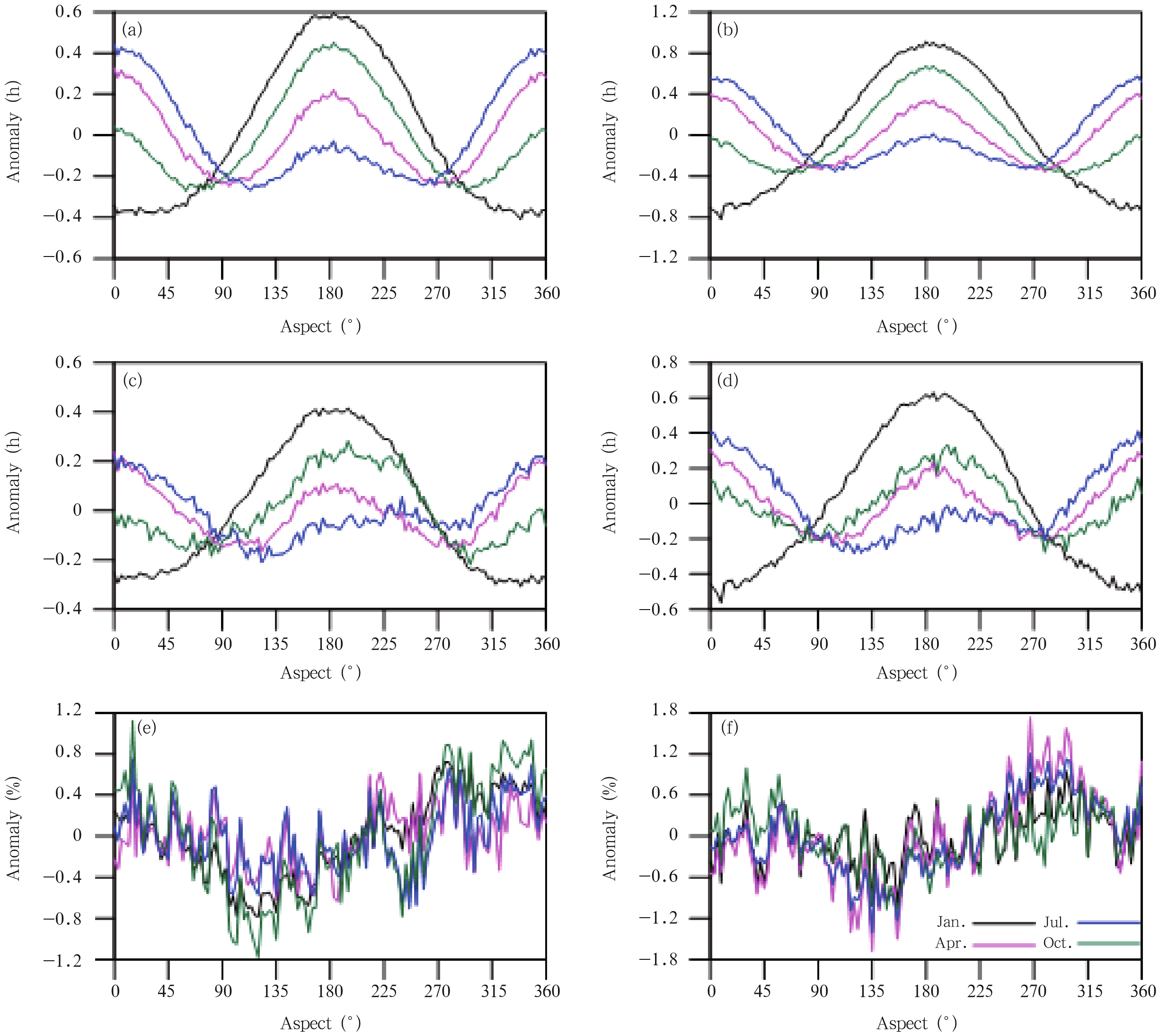

Fig. 7. Anomaly variation curves of (a, b) MPSD, (c, d) SD, and (e, f) cloud cover, associated with terrain slope aspect of (a, c, e) 10° and (b, d, f) 15°. The curve in black is for January, in purple for April, in blue for July, and in green for October.

Tropic of Capricorn, the maximum solar elevation angle is relatively small, and a general decreasing trend of SD was observed from south to north. The spatial difference for SD in the mountainous areas was obvious, and a large deviation in SD was observed between the south- and north-facing slopes.

5. Discussion

Several studies have used satellite data to estimate solar radiation (Tarpley, 1979; Gautier et al., 1980; Cano and Monget, 1986; Rigollier et al., 2004; Liu et al., 2008; Zhang and Wen, 2014). SD is strongly correlated with solar radiation, and it has been the most widely used variable to estimate solar radiation (Hu et al., 2010). Şahin et al. (2013) compared artificial neural network (ANN) and multiple linear regression (MLR) solar radiation estimation models in Turkey using NOAA/AVHRR data. Their results indicated that the ANN model achieved satisfactory performance compared to the MLR model. Moreover, satellite data improve the accuracy of solar radiation estimation results. Lu et al. (2011) proposed a simple and efficient algorithm to estimate the daily global solar radiation from geostationary satellite data. Their results demonstrated that the ANN model using geostationary satellite data showed acceptable accuracy with regard to both space and time.

We developed a remote sensing model to estimate SD using MODIS data. The annual average relative error was approximately 2.21%, and the relative interpolation error was approximately 7.90%. It is found that the use of satellite data to improve the model estimation accuracy led to significant improvement. Our model only requires the use of three commonly available data (i.e., DEM data, MODIS cloud cover data, and ground station observation data), and the acquisition of these data is generally feasible. Nonetheless, the current approach must be employed in more places to provide a more generalized SD estimation model.

SD is observed at meteorological stations and used to estimate solar radiation. The distribution of SD is significantly different in regions without meteorological stations or rugged mountains. Robaa (2008) developed three empirical formulae to estimate SD using readily available observational cloud cover data, which can only reflect the SD of these stations. Our estimation clearly reflects the distribution of SD, especially the SD estimates for rugged terrains. Hu et al. (2010) developed a calculation method for SD at any given point within natural canopy gaps. They primarily studied SD among natural canopy gaps, whereas we focused on SD estimation in rugged terrain areas. Şen and Öztopal (2003) presented a method to group solar irradiation/SD data into convenient seasonal subgroups, and then made quantitative predictions within each group. They sought to identify the biases caused in parameter estimates and to eliminate them with additional consideration in solar energy calculation.

6. Conclusions

Given the effects of terrain and atmospheric factors on SD, we used the Ningxia DEM data to provide comprehensive information about the local terrains, and used the MODIS cloud products for 2003 to simulate sunshine percentage and SD in this region. By applying this comprehensive SD model, we estimated the SD distributions in Ningxia and analyzed its seasonal and sub-regional variations. The major conclusions of this study are as follows:

(1) SD estimation is more accurate with the introduction of MODIS cloud data.

(2) The SD variation trend in Ningxia is consistent with that of the MPSD. The SD fluctuation is largely due to the effect of cloudy weather in April, July, and October; however, sunny days predominate in January, and the SD fluctuations in that month are relatively mild.

(3) The SD spatial variation is so substantial that the differences in the estimated SD between the south- and north-facing slopes are quite significant. Furthermore, the seasonal variation is also significant throughout the year.

The SD estimation method applied in this study only requires the use of three commonly available data (i.e., the DEM data, the MODIS cloud cover data, and the ground station observation data), and the acquisition of these data is generally feasible. Moreover, this estimation method could be of great significance for other areas of research, such as solar-resource assessment, surface-radiation numerical simulation, and surface energy balance research. This method might improve the accuracy and reliability of SD computation, and may be of great potential value in various solar energy related applications.

REFERENCES

Angstrom, A., 1924: Solar and terrestrial radiation. Report to the International Commission for Solar Research on actinometric investigations of solar and atmospheric radiation. *Quart. J. Roy. Meteor. Soc.*, **50**, 121–126.

Bertrand, C., C. Demain, and M. Journee, 2013: Estimating daily sunshine duration over Belgium by combination of station and satellite data. *Remote Sens. Lett.*, **4**, 735–744.

Bocquet, G., 1984: Method of study and cartography of the potential sunny periods in mountainous areas. *J. Climatol.*, **4**, 587–596.

Cano, D., J. M. Monget, M. Albuisson, et al., 1986: A method for the determination of the global solar radiation from meteorological satellite data. *Sol. Energy*, **37**, 31–39.

Cao Yun, He Yongjian, Qiu Xinfa, et al., 2012: Correction methods of MODIS cloud product based on ground observation data. *J. Remote Sens.*, **16**, 325–342.

Chen Hua, Sun Danfeng, Duan Zengqiang, et al., 2002: Sunshine hours modeling and spa-temporal variation analysis based on DEM in mountainous area—Take Mentougou mountain in West Beijing as the example. *J. Mountain Res.*, **20**, 559–563. (in Chinese)

Ding Shouguo, Zhao Chunsheng, Shi Guangyu, et al., 2005: Analysis of global total cloud amount variation over the past 20 years. *J. Appl. Meteor. Sci.*, **16**, 670–676. (in Chinese)

Dozier, J., and S. I. Outcalt, 1979: An approach toward energy balance simulation over rugged terrain. *Geographical Analysis*, **11**, 65–85.

Dubayah, R., J. Dozier, and F. W. Davis, 1990: Topographic distribution of clear-sky radiation over the Konza Prairie, Kansas. *Water Resour. Res.*, **26**, 679–690.

Ertekin, C., and F. Evrendilek, 2007: Spatio-temporal modeling of global solar radiation dynamics as a function of sunshine duration for Turkey. *Agr. Forest Meteor.*, **145**, 36–47.

Fu Baopu, 1958: Effects of sloping fields on sunshine and solar radiation. *J. Nanjing Univ. (Natural Science Edition)*, **2**, 23–46. (in Chinese)

Gautier, C., G. Diak, and S. Masse, 1980: A simple physical model to estimate incident solar radiation at the surface from GOES satellite data. *J. Appl. Meteor.*, **19**, 1005–1012.

Good, E., 2010: Estimating daily sunshine duration over the UK from geostationary satellite data. *Weather*, **65**, 324–328.

Hetrick, W. A., P. M. Rich, F. J. Barnes, et al., 1993: GIS-based solar radiation flux models. *ACSM-ASPRS Annual Convention*, **3**, 132–132.

Hu, L., B. Yan, X. Wu, et al., 2010: Calculation method for sunshine duration in canopy gaps and its application in analyzing gap light regimes. *For. Ecol. Manag.*, **259**, 350–359.

Kumar, L., A. K. Skidmore, and E. Knowles, 1997: Modeling topographic variation in solar radiation in a GIS environment. *Int. J. Geogr. Inf. Sci.*, **11**, 475–497.

Li Mengjie, Zheng Jianfei, Zeng Yan, et al., 2008: Distributed modeling of direct solar radiation over rugged terrains of Zhejiang Province. *Adv. Earth Sci.*, **23**, 299–305. (in Chinese)

Liu Ruixia, Chen Hongbin, Zheng Zhaojun, et al., 2009: Analysis and validation of total cloud amount data in China. *J. Appl. Meteor. Sci.*, **20**, 571–578. (in Chinese)

Liu Yonghong, Quan Weijun, Xia Xiangao, et al., 2008: Net surface solar radiation in the clear sky based on MODTRAN model and satellite data. *Plateau Meteor.*, **6**, 1410–1415.(in Chinese)

Lu, N., J. Qin, K. Yang, et al., 2011: A simple and efficient algorithm to estimate daily global solar radiation from geostationary satellite data. *Energy*, **36**, 3179–3188.

Matuszko, D., 2012: Influence of cloudiness on sunshine duration. *Int. J. Climatol.*, **32**, 1527–1536.

Moore, I. D., R. Grayson, and A. Ladson, 1991: Digital terrain modelling: A review of hydrological, geomorphological, and biological applications. *Hydrol. Processes*, **5**, 3–30.

Qiu Xinfa, Qiu Yueping, and Zeng Yan, 2009: Distributed modeling of monthly mean air temperature of rugged terrain of Chongqing. *Adv. Earth Sci.*, **24**, 621–628. (in Chinese)

Rigollier, C., M. Lefèvre, and L. Wald, 2004: The method Heliosat-2 for deriving shortwave solar radiation from satellite images. *Sol. Energy*, **77**, 159–169.

Robaa, S., 2008: Evaluation of sunshine duration from cloud data in Egypt. *Energy*, **33**, 785–795.

Şahin, M., Y. Kaya, and M. Uyar, 2013: Comparison of ANN and MLR models for estimating solar radiation in Turkey using NOAA/AVHRR data. *Adv. Space Res.*, **51**, 891–904.

Şen, Z., 2001: Angström equation parameter estimation by unrestricted method. *Sol. Energy*, **71**, 95–107.

Şen, Z., and A. Öztopal, 2003: Terrestrial irradiation-sunshine duration clustering and prediction. *Energ. Convers. Manage.*, **44**, 2159–2174.

Shamim, M. A., R. Remesan, D. W. Han, et al., 2012: An improved technique for global daily sunshine duration estimation using satellite imagery. *J. Zhejiang Univ. Sci. A*, **13**, 717–722.

Suehrcke, H., R. S. Bowden, and K. Hollands, 2013: Relationship between sunshine duration and solar radiation. *Sol. Energy*, **92**, 160–171.

Sun Hanqun and Fu Baopu, 1996: The elliptical integral model for computing the extra terrestrial solar radiation on mountain slopes. *Acta Geogr. Sin.*, **51**, 559–566. (in Chinese)

Takenaka, A., 1988: An analysis of solar beam penetration through circular gaps in canopies of uniform thickness. *Agr. For. Meteor.*, **42**, 307–320.

Tarpley, J. D., 1979: Estimating incident solar radiation at the surface from geostationary satellite data. *J. Appl. Meteor.*, **18**, 1172–1181.

Wang Yu, 1993: Vertical distribution of sunshine duration in mountainous areas of Yunnan Province. *J. Mountain Res.*, **11**, 1–8. (in Chinese)

Watson, R. T., and D. L. Albritton, 2001: *Climate Change 2001: Synthesis Report.* Third Assessment Report of the Intergovernmental Panel on Climate Change. Cambridge University Press, Cambridge, 408 pp.

Weng Duming, 1964: Overview of the climatological calculation methods of the total radiation. *Acta Meteor. Sinica*, **34**, 304–315. (in Chinese)

Weng Duming, Chen Wanglong, and Shen Juecheng, 1981: *Microclimate and Farmland Microclimate.* China Agriculture Press, Beijing, 357 pp. (in Chinese)

Weng Duming, 1997: *Studies on Radiation Climate of China.* China Meteorological Press, Beijing, 363 pp. (in Chinese)

Yin Hong, 1957: The use of empirical formula to calculate the total radiation distribution from the sunshine record in eastern China. *Acta Meteor. Sinica*, **28**, 101–107. (in Chinese)

Yuan Shujie, Miao Qilong, Qiu Xinfa, et al., 2008: The spatial and temporal distributions of insolation duration over rugged terrains in the Guizhou Plateau. *J. Appl. Meteor. Sci.*, **19**, 233–237. (in Chinese)

Zeng Yan, Qiu Xinfa, Miao Qilong, et al., 2003: Distribution of possible sunshine durations over rugged terrains of China. *Prog. Nat. Sci.*, **13**, 761–764.

Zhang Chungui and Wen Mingzhang, 2014: Using satellite data to estimate solar radiation of clear sky over Fujian. *J. Nat. Resour.*, **9**, 1496–1507. (in Chinese)

Zhu Zhihui, 1988: The global distribution of astronomical solar radiation on nonhorizontal surfaces. *Sci. China (Ser. B)*, **10**, 1100–1110.

Zuo Dakang, 1990: *Dictionary of Contemporary Geography.* The Commercial Press, Beijing, 863 pp. (in Chinese)